# Inviscid-Incompressible-Flow Theory of Normal and Slightly Oblique Impingement of a Static Round Jet on the Ground

T. STRAND*
*Air Vehicle Corporation, La Jolla, Calif.*

**An inviscid-incompressible-flow theory of normal and slightly oblique impingement of a static round jet on the ground is developed and compared with the results of a bench test. The velocity distribution along the ground and across the jet exit, the location of the free stream tube boundary, and thrust ratios at constant power and constant total head are presented as functions of the height of the jet exit above the ground and of the angle of tilt. The agreement between theory and experiment is satisfactory, except at very low height/diameter ratios.**

## Nomenclature

$A$ = a constant; also, cross-sectional area of jet exit
$B, C$ = constants
$D$ = jet exit diameter
$h$ = flow total head
$H$ = height of jet exit above ground
$I_0, I_1$ = Bessel functions of the first kind of first and second order, respectively
$p$ = static pressure
$P$ = power
$r$ = radial coordinate
$R$ = jet exit radius
$T$ = jet thrust (vertical force component)
$x$ = coordinate
$U$ = flow velocity
$v_x, v_r, v_\theta$ = velocity components
$\epsilon$ = angle of tilt
$\theta$ = angular coordinate
$\rho$ = air density
$\lambda$ = eigenvalue
$\mu$ = Lagrangian multiplier
$\Phi$ = velocity potential
$\varphi^{(b)}$ = basic potential
$\varphi^{(0)}, \varphi^{(1)}$ = perturbation potentials for normal and oblique impingement, respectively
$\psi$ = stream function

***Subscripts***

0 = ambient condition
1 = denotes radial extent of flow region under consideration

## I. Introduction

SEVERAL authors have in the past considered the mathematical problems associated with normal impingement of a round jet on a smooth surface. Essentially there exist only two methods of approach in ideal-fluid flow, namely, the method of singularities and the method of separation of variables. In the first method, singularities are distributed along the flow boundaries. This is the method used by Schach[1] to solve for the location of the boundary by successive approximations. After first assuming a shape for the unknown boundary, he calculated numerical values along this surface of a function that is zero if the boundary is the correct one. If the function is not zero, a new boundary is assumed and the process repeated. No rational basis was developed or shown for correcting the boundary shape.

Shen[2] used the method of separation of variables to expand the velocity potential in a series of Legendre polynomials, and satisfied the boundary condition in an average or weighted sense. He was thus able to reduce a double integral equation to a single integral equation. If trial and error techniques were not to be used for finding the unknown boundary, Shen indicated that the alternative involved the solution of simultaneous nonlinear algebraic equations. Solution of these was not attempted.

A semiempirical method, involving determination of the shape of the free boundary using an electrolytic analog tank, was developed by LeClerc.[3] He then computed the internal flow numerically, using relaxation methods.

The foregoing authors employed trial and error techniques to determine the shape of the free stream tube. Later, Ludwig and Brady[4,5] tried a systematic iterative approach for determination of the unknown boundary using the method of singularities. Convergence of the method was found to be very slow, however. For a given jet height/diameter ratio the computation required approximately 70 iterations and about 4 hr of computing time on a high-speed digital computer (IBM 704). Recently, Tani and Komatsu[6] developed a semiempirical procedure for constructing the velocity field from a knowledge of the velocity distribution along the jet centerline.

No solutions are known for the case of oblique impingement. In the subsequent pages, a systematic iterative approach, using the method of separation of variables combined with small perturbation theory, will be presented. Instead of the spherical harmonics used by Shen, cylindrical harmonics are employed.

It has been established experimentally that the jet flowfield may be divided into three regions, namely, 1) the free jet region, at heights greater than approximately two jet exit diameters above the ground (in this region essentially no influence of the ground can be detected); 2) the impingement region, in which the flow turns through 90°; and 3) the wall jet region at radii greater than approximately one diam (in this region the jet flows radially over the ground with essentially zero pressure gradient). The free jet and the wall jet regions are mainly influenced by viscous forces, and may be considered adequately covered by theory. The present investigation is concerned with the impingement region, in which pressure and momentum forces dominate, provided the jet exit is not too far removed from the ground. It represents a further development of the results given in Ref. 7.

## II. Theory

### A. Expansion of the Velocity Potential

We shall investigate a steady irrotational flow of an inviscid-incompressible fluid. The governing partial differ-

Received February 3, 1967; revision received May 24, 1967. The research was supported by the U.S. Army Research Office-Durham under Contract DA-31-124-ARO-D-311. The author is indebted to P. M. Yager for programming the method on the digital computer, and for several helpful suggestions. [3.01]

* President of company. Associate Fellow AIAA.

ential equation of such a flow is Laplace's equation, which in cylindrical coordinates $(x, r, \theta)$ can be written in the form

$$\Phi_{xx} + \Phi_{rr} + (1/r)\Phi_r + (1/r^2)\Phi_{\theta\theta} = 0 \quad (1)$$

Here $\Phi$ denotes the velocity potential defined by the components $v_x$, $v_r$, $v_\theta$ of the velocity $U$ at an arbitrary point in the flow, as follows:

$$\left.\begin{aligned} v_x &= \Phi_x \\ v_r &= \Phi_r \\ v_\theta &= (1/r)\Phi_\theta \end{aligned}\right\} \quad v_x^2 + v_r^2 + v_\theta^2 = U^2 \quad (2)$$

The subscripts of the potential indicate partial differentiation. The origin of the cylindrical coordinate system is shown in Fig. 1.

Letting the angle of tilt $\epsilon$ of the jet be small, we shall assume that the velocity potential may be expanded in a series of the form

$$\Phi = \varphi^{(b)}(x,r) + \varphi_0^{(0)}(x,r) + \sum_{n=1}^{\infty} \epsilon^n \varphi^{(n)}(x,r,\theta) \quad (3)$$

Here $\varphi^{(b)}$ denotes a known basic solution, which almost, but not quite, satisfies all the boundary conditions. The $\varphi^{(n)}$'s are perturbation potentials. Both $\varphi^{(b)}$ and $\varphi^{(n)}$ are themselves, in general, series expansions, although in order to get started on an iteration procedure for determining the location of the free stream tube, the initial expression for $\varphi^{(b)}$ will consist of only a single term (see below).

### B. Boundary Conditions

The following boundary conditions will be imposed upon the jet flowfield:

1) $v_x = 0$ for $x = H$ (Fig. 1), i.e., the flow component normal to the ground is zero.

2) $v_r^2 + v_\theta^2 = (U_0\epsilon)^2$ for $x = 0$, i.e., there is a constant sidewise velocity component equal to $U_0\epsilon$ in the plane of the jet exit. Here $U_0$ and $\epsilon$ denote, respectively, the constant velocity corresponding to ambient pressure and the angle of tilt of the jet. The plane $x = 0$ will always be assumed to be the plane of the jet exit, even in the case of a slight nozzle tilt.

3) $U = U_0$ along the free stream tube (Fig. 1).

4) $U = U_0$ along a cylindrical surface $(x,r_1)$, defining the maximum radial extent of the flow region under consideration, and the start of the wall jet region.

### C. Basic Solution

To employ small perturbation theory, it is first necessary to find a basic solution for normal impingement ($\epsilon = 0$) which almost, but not quite, satisfies all boundary conditions of the flow region. In the case of normal impingement, the governing expression is Eq. (1) with the last term on the left-hand side of the equal sign omitted. By the method of separation of variables it is easily shown that a possible solution, which yields finite velocities along the jet centerline ($r = 0$), is

$$\varphi^{(b)} = AU_0HI_0(\pi r/2H)\sin(\pi x/2H) \quad (4)$$

Here $A$ is an arbitrary constant, and $H$ is the height of the jet exit above the ground. $I_0$ denotes the modified Bessel function of the first kind of the zeroth order. This basic solution automatically satisfies boundary conditions B.1 and B.2 of the previous section.

The corresponding stream function may be shown to be

$$\psi^{(b)} = CrI_1(\pi r/2H)\cos(\pi x/2H) \quad (5)$$

where $C$ is an arbitrary constant, and $I_1$ is the modified Bessel function of the first kind of the first order. Substitution of the point $(0,R)$ into Eq. (5) yields the following implicit relation for the rim stream tube

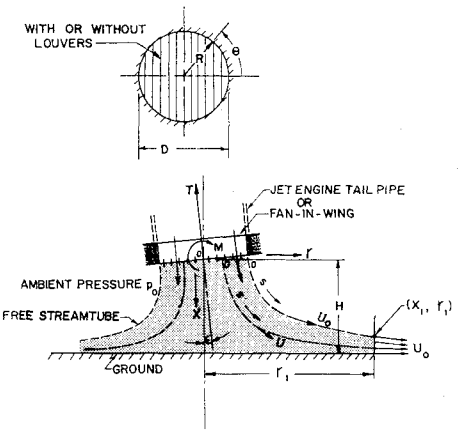


**Fig. 1 Coordinate system of slanted jet in ground proximity.**

$$rI_1(\pi r/2H)\cos(\pi x/2H) = RI_1(\pi R/2H) \quad (6)$$

Solving for $x$, we obtain a first estimate for the location of the free stream tube, i.e.,

$$\frac{x}{H} = \frac{2}{\pi}\cos^{-1}\left[\frac{(R/H)I_1(\pi R/2H)}{(r/H)I_1(\pi r/2H)}\right] \quad (7)$$

The flow velocity squared along this boundary is obtainable to within an unknown constant by differentiating Eq. (4) with respect to $x$ and $r$, and then squaring and summing the two terms. The value of the unknown constant $A$ may be selected so as to yield the best fit to $U_0^2$ of this function along the boundary given by Eq. (7). In most cases it was only necessary to determine $A$ by setting $\varphi_x^{(b)} = U_0$ at the rim point $(0,R)$. This yields $A = 2/\pi\ I_0(\pi R/2H)$.

### D. Perturbation Potentials

Again, by the method of separation of variables, we can show that possible solutions of Eq. (1), which satisfy boundary conditions B.1 and B.2, and yield finite velocities along the line $r = 0$, are the perturbation potentials

$$\varphi^{(0)} = U_0H\sum_{n=0}^{\infty} A_nI_0(\lambda_n r)\sin(\lambda_n x) \quad (8)$$

$$\varphi^{(1)} = U_0\cos\theta\left[r + H\sum_{n=0}^{\infty} B_nI_1(\lambda_n r)\sin(\lambda_n x)\right] \quad (9)$$

with $\lambda_n = (1 + 2n)\pi/2H$, where $n = 0, 1, 2 \ldots$. Here $A_n$ and $B_n$ indicate unknown constants. The first term on the right-hand side of Eq. (9), when multiplied by $\epsilon$ [see Eq. (3)], is seen to be the potential of a uniform stream of velocity $U_0\epsilon$ parallel to the ground.

### E. Constant Pressure Boundary Condition

To linearize the constant pressure condition along the free stream tube and along the cylindrical bounding surface, the expression for the velocity squared at an arbitrary point in the flowfield is needed. Through use of Eqs. (2) and (3) we may write

$$v_x^2 + v_r^2 + v_\theta^2 = \left[\varphi_x^{(b)} + \sum_{n=0}^{\infty}\epsilon^n\varphi_x^{(n)}\right]^2 + \left[\varphi_r^{(b)} + \sum_{n=0}^{\infty}\epsilon^n\varphi_r^{(n)}\right]^2 + \left[\frac{1}{r}\sum_{n=1}^{\infty}\epsilon^n\varphi_\theta^{(n)}\right]^2 \quad (10)$$

Constant pressure along a stream tube implies constant velocity squared by Bernoulli's equation. Thus, setting the left-hand side of Eq. (10) equal to $U_0^2$ corresponding to

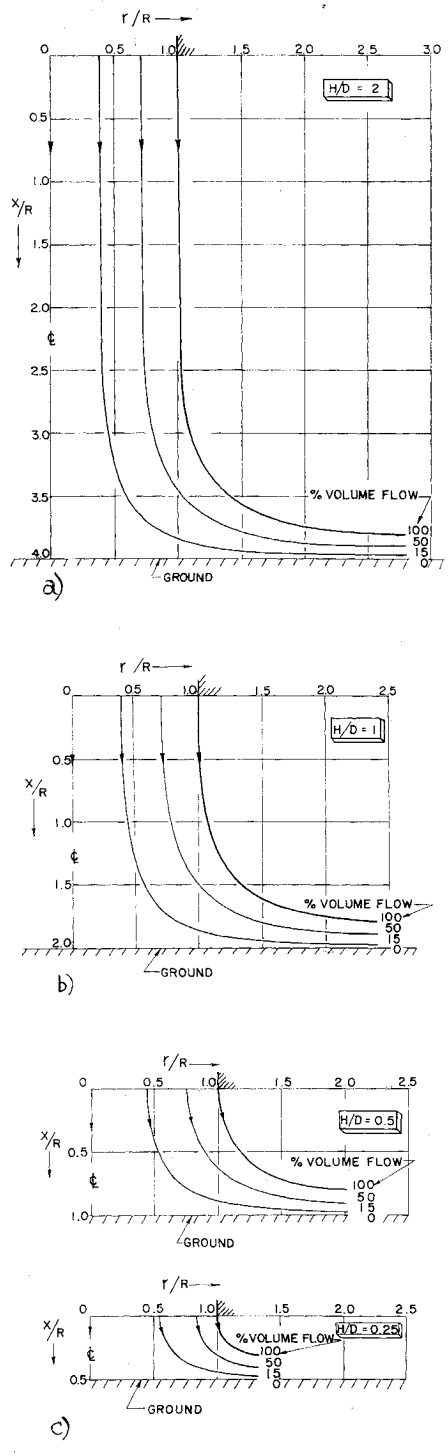


**Fig. 2 Stream tube shapes for impingement normal to the ground.**

ambient pressure, and rewriting the right-hand side, we find

$$\tfrac{1}{2}[U_0^2 - \varphi_x^{(b)2} - \varphi_r^{(b)2}] = \varphi_x^{(b)}\varphi_x^{(0)} + \varphi_r^{(b)}\varphi_r^{(0)} + \text{higher order terms} + \epsilon\{[\varphi_x^{(b)} + \varphi_x^{(0)}]\varphi_x^{(1)} + [\varphi_r^{(b)} + \varphi_r^{(0)}]\varphi_r^{(1)} + \text{higher order terms}\} + \epsilon^2\{\ldots.\} + \ldots. \quad (11)$$

This expression must hold for all angles of tilt along the two boundaries where the velocity equals $U_0$. The coefficients of each power of $\epsilon$ must therefore be set equal to zero. The result is a sequence of equations, the first two of which are

$$\varphi_x^{(b)}\varphi_x^{(0)} + \varphi_r^{(b)}\varphi_r^{(0)} - \tfrac{1}{2}[U_0^2 - \varphi_x^{(b)2} - \varphi_r^{(b)2}] = 0 \quad (12)$$

$$[\varphi_x^{(b)} + \varphi_x^{(0)}]\varphi_x^{(1)} + [\varphi_r^{(b)} + \varphi_r^{(0)}]\varphi_r^{(1)} = 0 \quad (13)$$

The nonlinear condition along the free stream tube and along the bounding cylindrical surface of radius $r_1$ has now been replaced, to the first order in the angle of tilt $\epsilon$, by the preceding two linear equations. These equations show that we should first solve the problem of impingement normal to the ground, the boundary condition of which is given by Eq. (12). After this solution is in hand, we may then obtain the perturbation potential due to tilt, using Eq. (13).

Equations (12) and (13) may be satisfied either by collocation or by the method of least squares. Here we shall use the method of least squares since it, by experience, yields more satisfactory results. Letting $s$ be the distance along any stream tube at constant $\theta$, measured from an initial point in the jet exit plane ($x = 0$), we now define two new functions $f$ and $g$, the integrands of which are given by the left-hand sides of Eqs. (12) and (13), as follows

$$f[\varphi^{(0)}] = \int_0^{s_1} \left\{\varphi_x^{(b)}\varphi_x^{(0)} + \varphi_r^{(b)}\varphi_r^{(0)} - \frac{1}{2} \times [U_0^2 - \varphi_x^{(b)2} - \varphi_r^{(b)2}]\right\}^2 ds + \int_{x_1}^{H} \left\{\varphi_x^{(b)}\varphi_x^{(0)} + \varphi_r^{(b)}\varphi_r^{(0)} - \frac{1}{2}[U_0^2 - \varphi_x^{(b)2} - \varphi_r^{(b)2}]\right\}^2 dx \quad (14)$$

$$g[\varphi^{(1)}] = \int_0^{s_1} \{[\varphi_x^{(b)} + \varphi_x^{(0)}]\varphi_x^{(1)} + [\varphi_r^{(b)} + \varphi_r^{(0)}]\varphi_r^{(1)}\}^2 ds + \int_{x_1}^{H} \{[\varphi_x^{(b)} + \varphi_x^{(0)}]\varphi_x^{(1)} + [\varphi_r^{(b)} + \varphi_r^{(0)}]\varphi_r^{(1)}\}^2 dx \quad (15)$$

Here the subscript 1 denotes a point of intersection of the free stream tube with the cylindrical surface of radius $r_1$ for the case of impingement normal to the ground. The distance to this point along the bounding stream tube is given by $s_1$. The two functions $f$ and $g$ are measures of how well the linearized boundary conditions [Eqs. (12) and (13)] are satisfied along the constant pressure boundary.

Because we know the direction of the velocity vector at the two end points $(0,R)$ and $(H,r_1)$, we may also introduce Lagrangian multipliers $\mu_1$, $\mu_2$, $\mu_3$, and $\mu_4$, to further tie down the velocities at these points. We therefore define two additional functions $F$ and $G$, i.e.,

$$F[\varphi^{(0)}] = f + \mu_1[\varphi_x^{(b)}(0,R) + \varphi_x^{(0)}(0,R) - U_0] + \mu_2[\varphi_r^{(b)}(H,r_1) + \varphi_r^{(0)}(H,r_1) - U_0] \quad (16)$$

$$G[\varphi^{(1)}] = g + \mu_3\varphi_x^{(1)}(0,R) + \mu_4\varphi_r^{(1)}(H,r_1) \quad (17)$$

where $\varphi^{(0)} = \varphi^{(0)}(A_n)$ and $\varphi^{(1)} = \varphi^{(1)}(B_n)$. The extrema of $f$ and $g$ are obtained when the functions $F$ and $G$ fulfill the two separate sets of equations

$$\partial F/\partial A_n = \partial F/\partial \mu_1 = \partial F/\partial \mu_2 = 0 \quad (18)$$

$$\partial G/\partial B_n = \partial G/\partial \mu_3 = \partial G/\partial \mu_4 = 0 \qquad n = 0, 1, 2, \ldots \quad (19)$$

The foregoing expressions form a determined system of linear algebraic equations for the determination of $A_n$, $B_n$, and $\mu_1, \ldots, \mu_4$ if a partial sum is taken in Eqs. (8) and (9), and provided the approximate location of the free stream tube for the case of impingement normal to the ground is known. Note that we intend to satisfy the boundary condition for oblique impingement [Eq. (13)] in the sense of least squares along a known boundary to be calculated for the case of normal impingement. The perturbation potential due to oblique impingement is thus determined without iteration.

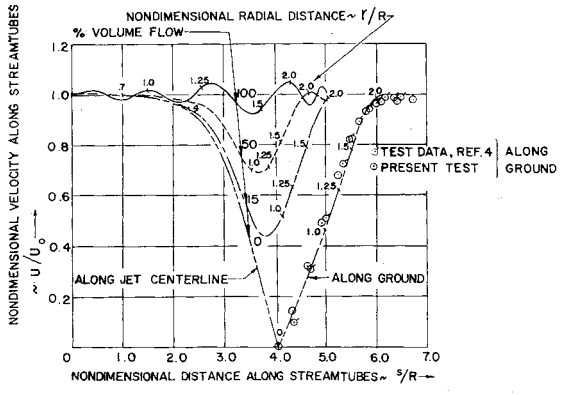


**Fig. 3 Flow velocities along stream tubes for impingement normal to the ground for $H/D = 2$.**

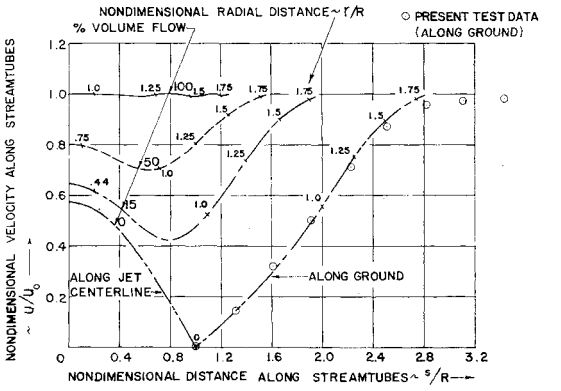


**Fig. 5 Flow velocities along stream tubes for impingement normal to the ground for $H/D = 0.5$.**

### F. The Iterative Method

The stream tubes for normal impingement corresponding to the velocity potentials given by Eqs. (4) and (8) are easily calculated from the stream function $\psi$, where

$$\psi = 2\pi r \int_x^H [\Phi_r]_{r=\text{const}}\, dx \sim$$

$$ArI_1(\lambda_0 r)\cos(\lambda_0 x) + r\sum_{n=0}^{m} A_n I_1(\lambda_n r)\cos(\lambda_n x) \quad (20)$$

by specifying the originating point of the stream tube in the jet exit plane. Thus, when the point at the rim $(0,R)$ is specified, we find

$$ArI_1(\lambda_0 r)\cos(\lambda_0 x) + r\sum_{n=0}^{m} A_n I_1(\lambda_n r)\cos(\lambda_n x) =$$

$$ARI_1(\lambda_0 R) + R\sum_{n=0}^{m} A_n I_1(\lambda_n R) \quad (21)$$

With the coefficients $A_n$ obtained by solving the matrix Eq. (18), this is an implicit expression for the location of the bounding stream tube, i.e., by choosing a value for $x$ we may calculate the corresponding radius $r$. If the method works, a closer approximation to the true constant pressure stream tube than that given by Eq. (7) will now have been obtained.

The new location of the stream tube is next inserted in the matrix Eq. (18) for the second solution of the same equation. The new basic potential that corresponds to the new location of the free stream tube is given by

$$\varphi^{(b)} = HU_0 AI_0(\lambda_0 r)\sin(\lambda_0 x) +$$

$$HU_0\sum_{n=0}^{m} A_n^{(1)} I_0(\lambda_n r)\sin(\lambda_n x) \quad (22)$$

Here the superscript of the coefficients indicates that the values are obtained from the first iteration. The convergence of the method was found to be quite rapid, provided the bounding cylindrical surface of radius $r_1$ was not chosen too far from the jet centerline. Beyond a limiting $r_1$, convergence could not be obtained.

The final free stream tube for normal impingement was then used in the solution of the matrix equation for oblique impingement, Eq. (19). It should possibly be mentioned that in order to more nearly equalize the sizes of the unknown coefficients, each $n$th term in the series expansion of the potentials [Eq. (8) and (9)] was arbitrarily divided by the constant factor $I_0(\lambda_n R)$.

### G. Calculated Results

The method developed in the preceding pages was programmed on the CDC-3600 digital computer at the University of California, San Diego. Stream tube shapes obtained from this program for the case of impingement normal to the ground for $H/D = 2$, 1, 0.5, and 0.25 are presented in Figs. 2a, b, and c. The magnitudes of the velocity vectors along the same stream tubes are given in nondimensional form in Figs. 3–6 as functions of the downstream distance $s$, measured from the jet exit plane. A 10-term series expansion was used. The velocities along the jet centerline ($s = x$) and along the ground ($s = H + r$) are included in these figures. It is noted in Fig. 3 that the magnitude of the nondimensional velocity along the bounding stream tube (100% volume flow) oscillates on both sides of the true value of unity, with a maximum error of −7 and +5% indicated for $H/D = 2$. With the jet exit closer to the ground, the excursions from the given boundary condition are considerably smaller, as seen in Figs. 4–6. The amplitude of the oscillations could be further reduced by employing more terms in the series

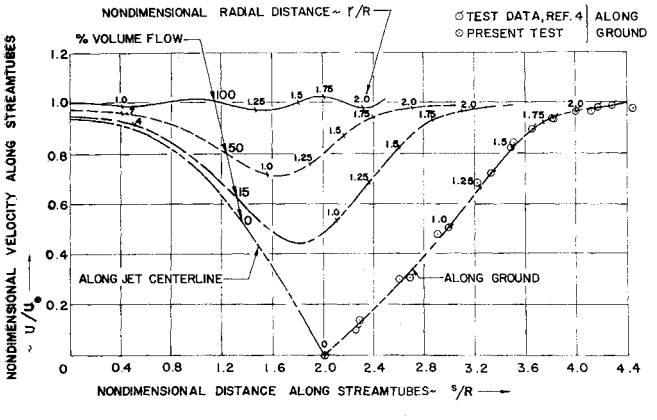


**Fig. 4 Flow velocities along stream tubes for impingement normal to the ground for $H/D = 1$.**

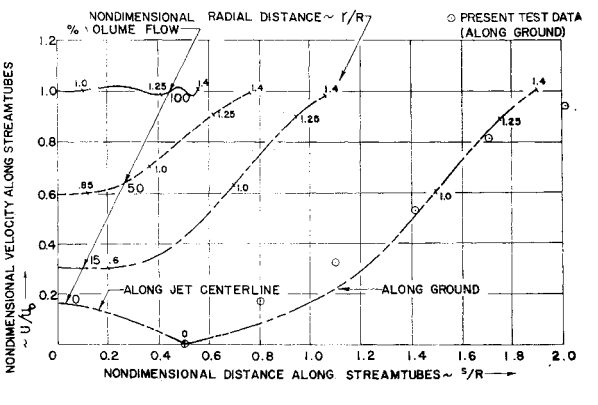


**Fig. 6 Flow velocities along stream tubes for impingement normal to the ground for $H/D = 0.25$.**

**Table 1 Coefficients in series expansion**

$A_nI(\lambda_nR)$

| | $n$ | | | | | | | | | |
|---|---|---|---|---|---|---|---|---|---|---|
| $H/D$ | 0 | 1 | 2 | 3 | 4 | 5 | 6 | 7 | 8 | 9 |
| 2 | 2.526 | −0.279 | 0.064 | −0.010 | $-2.459\cdot10^{-3}$ | $6.684\cdot10^{-3}$ | $-1.960\cdot10^{-3}$ | $-2.640\cdot10^{-3}$ | $-6.627\cdot10^{-3}$ | $-5.289\cdot10^{-5}$ |
| 1 | 0.829 | −0.067 | −0.004 | $3.699\cdot10^{-3}$ | $4.002\cdot10^{-4}$ | $-1.581\cdot10^{-4}$ | $-4.829\cdot10^{-5}$ | $-5.681\cdot10^{-6}$ | $-3.228\cdot10^{-7}$ | $-7.362\cdot10^{-9}$ |
| 0.5 | −0.009 | 0.008 | −0.002 | $-4.896\cdot10^{-4}$ | $-7.020\cdot10^{-5}$ | $-6.772\cdot10^{-6}$ | $-4.500\cdot10^{-7}$ | $-1.994\cdot10^{-8}$ | $-5.363\cdot10^{-10}$ | $-6.691\cdot10^{-12}$ |
| 0.25 | −0.365 | 0.013 | 0.001 | $1.673\cdot10^{-4}$ | $1.652\cdot10^{-5}$ | $1.300\cdot10^{-6}$ | $7.786\cdot10^{-8}$ | $3.352\cdot10^{-9}$ | $9.372\cdot10^{-11}$ | $1.303\cdot10^{-12}$ |

$B_nI_0(\lambda_nR)$

| | $n$ | | | | | | | | | |
|---|---|---|---|---|---|---|---|---|---|---|
| $H/D$ | 0 | 1 | 2 | 3 | 4 | 5 | 6 | 7 | 8 | 9 |
| 2 | −0.222 | 0.042 | −0.021 | $7.744\cdot10^{-3}$ | $-2.399\cdot10^{-3}$ | $-1.735\cdot10^{-3}$ | $1.897\cdot10^{-3}$ | $1.218\cdot10^{-3}$ | $2.467\cdot10^{-4}$ | $1\ 729\cdot10^{-5}$ |
| 1 | −0.268 | 0.055 | −0.006 | $-1.943\cdot10^{-3}$ | $9.939\cdot10^{-4}$ | $4.725\cdot10^{-4}$ | $8.633\cdot10^{-5}$ | $8.341\cdot10^{-6}$ | $4.241\cdot10^{-7}$ | $8.990\cdot10^{-9}$ |

expansion. The 10 terms used must be considered a compromise between the conflicting requirements of high accuracy in fulfilling the free stream tube boundary condition and low cost of digital computer time. The coefficients in the series are presented in Table 1.

The calculated velocity distributions along a radius in the jet exit plane for the case of normal impingement are shown in Fig. 7. It is seen that the effect of ground proximity is starting to show up at around $H/D = 1$. When the height is lowered below this value, there is a progressive decrease in the velocity in the central portion of the jet exit. Thus, if the jet total head remains constant at all heights, ground effect causes a reduction in jet volume flow as the height is decreased. For $H/D \geq 2$ (approximately) the jet exit velocity distribution is essentially uniform, and no effect of the ground can be detected.

By passing a horizontal momentum control surface through the origin, it may be shown that the vertical jet thrust $T$ is expressed by the following integral, valid for both normal and oblique impingement in our case:

$$T = \int_0^{2\pi}\int_0^R [p - p_0 + \rho\Phi_x{}^2]_{x=0}\, r dr d\theta = \pi\rho U_0{}^2 \int_0^R \{1 + [\varphi_x{}^{(b)}/U_0 + \varphi_x{}^{(0)}/U_0]^2\}_{x=0}\, r dr \quad (23)$$

Here $p$ is the pressure at any point. The subscript 0 denotes ambient condition. To the order of approximation used in this analysis, the thrust therefore remains unchanged by a small amount of jet tilt. The thrust of the jet, when far removed from the ground, is

$$T_{H=\infty} = \pi R^2 \rho U_{0H=\infty}{}^2 \quad (24)$$

If now the jet total head is maintained constant as the ground is approached (i.e., if $U_0 = U_{0H=\infty}$), we find by dividing Eq. (23) by Eq. (24) that

$$\frac{T}{T_{H=\infty}} = \frac{1}{R^2}\int_0^R \{1 + [\varphi_x{}^{(b)}/U_0 + \varphi_x{}^{(0)}/U_0]^2\}_{x=0}\, r dr \quad (25)$$

If, however, the power $P$ is maintained constant instead of the total head, we have

$$\frac{P}{P_{H=\infty}} = \frac{\pi\rho U_0{}^3 \int_0^R [\varphi_x{}^{(b)}/U_0 + \varphi_x{}^{(0)}/U_0]_{x=0}\, r dr}{\pi R^2 \rho U_{0H=\infty}{}^3} = 1 \quad (26)$$

from which we may solve for the required velocity ratio for constant power:

$$\frac{U_0}{U_{0H=\infty}} = \left\{\frac{1}{R^2}\int_0^R [\varphi_x{}^{(b)}/U_0 + \varphi_x{}^{(0)}/U_0]_{x=0}\, r dr\right\}^{-1/3} \quad (27)$$

By inspection (Fig. 7), this ratio is in ground proximity always larger than unity, and increases as the ground is approached. To maintain constant power as the height above the ground is decreased, it is therefore necessary to gradually increase the total head of the flow.

Substitution of Eq. (27) into Eq. (23) and use of Eq. (24) yields the thrust ratio at constant power:

$$\frac{T}{T_{H=\infty}} = \frac{\frac{1}{R^2}\int_0^R \{1 + [\varphi_x{}^{(b)}/U_0 + \varphi_x{}^{(0)}/U_0]^2\}_{x=0}\, r dr}{\left\{\frac{1}{R^2}\int_0^R [\varphi_x{}^{(b)}/U_0 + \varphi_x{}^{(0)}/U_0]_{x=0}\, r dr\right\}^{2/3}} \quad (28)$$

The two expressions for thrust ratio [Eqs. (25) and (28)] are plotted in Fig. 8. It is seen that the curve for constant power shows an initial decrease of about 5% as the ground is approached, indicating a suck-down of the aircraft, and

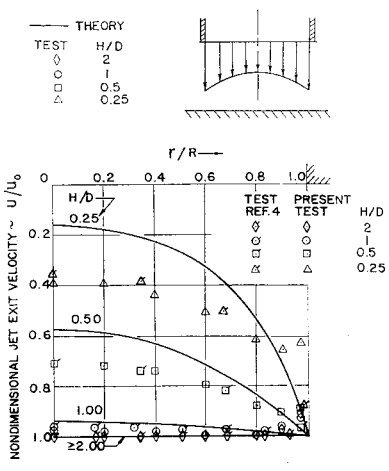


**Fig. 7 Velocity distribution in the plane of the jet exit for impingement normal to the ground.**

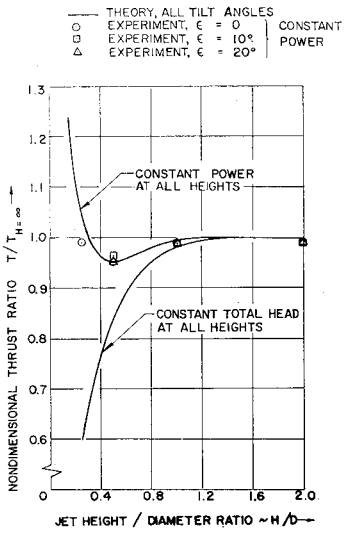


**Fig. 8 Thrust variation in ground proximity.**

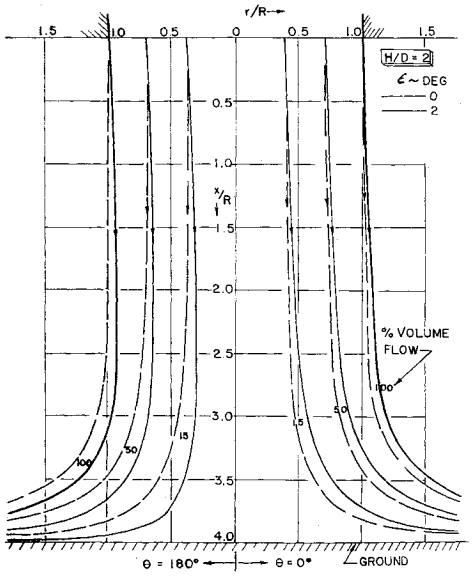


**Fig. 9 Comparison of stream tube shapes for normal and oblique impingement.**

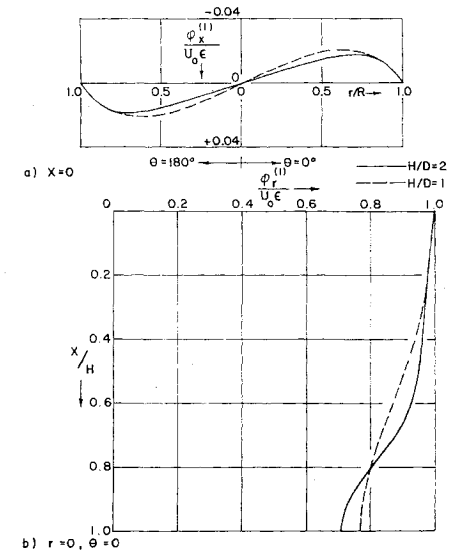


**Fig. 10 Perturbation velocities due to tilt.**

then rises to very large values with further decreases in ground clearance. The curve for constant total head, on the other hand, shows a monotonic thrust decrease as the ground is approached.

For oblique impingement the stream lines may be calculated by a stepwise integration of the local flow direction, since in this case a stream function does not exist. A typical result of such in integration is presented in Fig. 9 for $H/D = 2$. Here calculated stream lines in the plane of symmetry of the jet for $\epsilon = 2°$ are compared with those for normal impingement.

Calculated perturbation velocities across the jet exit in the plane of symmetry are shown in Fig. 10a for oblique impingement at $H/D = 2$ and 1. The perturbations are exceedingly small, and it is possible that they would vanish altogether if an iteration method for oblique impingement could be devised. Without iteration, as shown, they indicate that a small stabilizing pitching moment should be acting on the jet. The subsequent experimental results showed zero pitching moment at these heights. Improved theory or improved test instrumentation would be required to determine if a stabilizing moment really exists.

The horizontal perturbation velocities along the line $r = 0$ for the case of oblique impingement are given in Fig. 10b. The vertical perturbation velocities due to oblique impingement are zero along this line, as may be seen by inspection of Eq. (9).

Figures 11a and b show calculated velocity distributions along the ground in the plane of symmetry of the jet for $H/D = 2$ and 1 with $\epsilon = 0$ and 10°. The ground stagnation point for the case $\epsilon = 10°$ has been translated so as to coincide with that for $\epsilon = 0$.

It should be noted that although the theory for normal impingement is supposed to be applicable for all jet height/diameter ratios, this is not the case for the theory of oblique impingement. In deriving this latter theory, a boundary condition of constant sidewise velocity components at each point in the jet exit plane was imposed. This is a valid condition for those heights at which the influence of the ground is not felt in the jet exit, i.e., for uniform jet exit distribution ($H/D \geq 1$ approximately).

## III. Experiments

To determine if the theoretical results could be verified experimentally, a small subcontract for a bench test was placed with General Dynamics/Convair. A 4-in.-diam plant-air supply line delivered compressed air to a plenum chamber. A 3.3-in.-i.d., 17-in.-long aluminum cylinder with a bell-mouth inlet was inserted into the plenum chamber. The air from the cylinder impinged on a 6- × 6-ft ground board that could be adjusted in height and tilt.

All tests were run at a constant flow power of 1074.4 ft lb/sec (1.95 hp). The weight flow was determined by means of an orifice-type flow meter fitted with a 3-in.-diam orifice plate in the 4-in.-diam supply line. The pressure distribution across the jet exit was surveyed with a movable pitot-static probe. Total and static pressures were measured in pounds/square inch by means of a differential pressure transducer connected to the probe. An $X$-$Y$ plotter was used to record the pressure distributions for each straight-line sweep through the jet exit. The recorded total head pressure was constant across the jet exit to ±2%. The boundary-layer thickness at the jet exit was of the order of 10–15% of the radius. $U_0$ for the exit velocity profiles was calculated for each height from the total head pressure (gage) recorded in the jet exit.

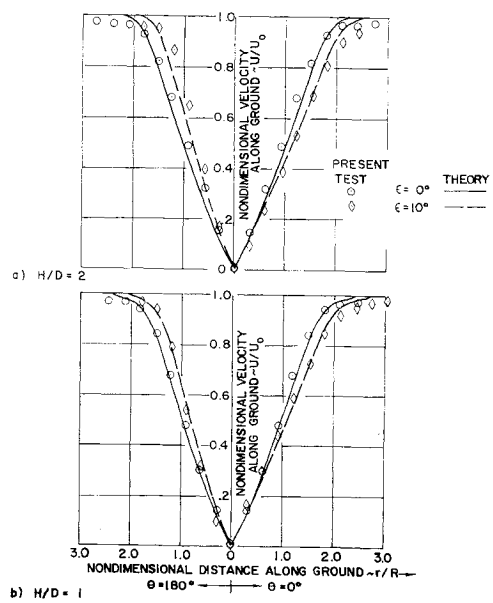


**Fig. 11 Velocities along the ground for normal and oblique impingement (stagnation point translated for $\epsilon = 10°$).**

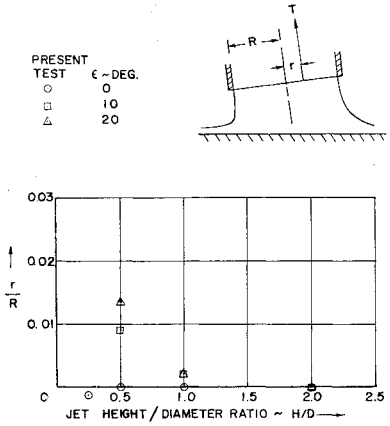


**Fig. 12 Destabilizing pitching moment.**

The ground velocity distribution was obtained from static pressure taps located with $\frac{1}{2}$-in. spacing in the ground plate in the plane of symmetry of the jet. A reference $U_0$ was calculated here from the recorded pressure at the ground stagnation point.

The experimentally determined velocity distributions along the ground for normal impingement are plotted in Figs. 3–6, and, except at $H/D = 0.25$ (Fig. 6), generally show excellent agreement with theory. It may be conjectured that at very low heights the imposed boundary condition of zero radial velocity components in the exit plane (boundary condition B.2) is not valid any longer. The flow probably does have nonzero radial velocity components in the jet exit plane at very low height/diameter ratios. Or, another possibility for the discrepancy between theory and experiment at very low heights might be sought in the intensified viscous phenomena taking place just outside the free stream tube. It was noticed in the tests that the static pressure at the rim of the jet exit was far from equal to the ambient pressure as assumed in the theory at $H/D = 0.25$. The rim pressure was considerably higher than ambient (of the order of the middle between the ambient and the jet total head pressures), indicating the existence of a strong viscous ring vortex surrounding the free stream tube. Thus part of the air in the jet would recirculate and increase the outside pressure felt by the issuing flow. This type of vortex has been observed earlier in connection with ground effect machines. Whatever the cause may be, the test results establish a lower height limitation on the validity of the present theory for the case of normal impingement.

The experimentally determined velocity distributions across the jet exit are shown in Fig. 7. It is noted that the discrepancy between test results and theory becomes progressively worse as the ground clearance is decreased.

The thrust at each ground height was calculated from the measured total and static pressures in the jet exit from the equation

$$T = \int (h - p_0) dA + \int (h - p) dA \qquad (29)$$

where $h$ and $p$ denote total head and local static pressures, respectively, and $A$ is the cross-sectional area. This equation is equivalent to Eq. (23). The results are presented in Fig. 8, and show good agreement with theory. This might be considered somewhat fortuitous at very small heights in view of the comments in the previous paragraph.

The measured velocity distributions along the ground are shown in Fig. 11 for $\epsilon = 0°$ and $\epsilon = 10°$ with $H/D = 2$ and 1. Good agreement with theory is noted.

Finally, in Fig. 12 experimental points are shown which indicate that a destabilizing pitching moment acts on the tilted jet exit structure at $H/D < 1$. A corresponding theoretical curve is not available, because the present theoretical development essentially assumes uniform flow across the jet exit when the jet is tilted.

## References

[1] Schach, W., "Deflection of a circular fluid jet by a flat plate perpendicular to the flow direction," Ing. Arch. **VI**, 51–59 (1935).

[2] Shen, Y. C., "Theoretical analysis of jet-ground plane interaction," Institute of Aerospace Science Paper 62–144 (June 1962).

[3] LeClerc, A., "Deflection of a liquid jet by a perpendicular boundary," M.S. thesis, State Univ. of Iowa (1948).

[4] Brady, W. G. and Ludwig, G. R., "Theoretical and experimental studies of impinging uniform jets," Transportation Research Command TR 63–11 AD 408, 669 (April 1963).

[5] Ludwig, G. R. and Brady, W. G., "Theoretical and experimental studies of impinging uniform and nonuniform jets," Transportation Research Command TR 64–42, AD 61063 (August 1964).

[6] Tani, I. and Komatsu, Y., "Impingement of a round jet on a flat surface," *Applied Mechanics, Proceedings of the Eleventh International Congress of Applied Mechanics*, edited by H. Görtler (Springer Verlag, Berlin, 1964).

[7] Strand, T., "On the theory of normal ground impingement of axisymmetric jets in inviscid incompressible flow," AIAA Paper 64–424 (1964).